Mukherjee et al., http://www.jgp.org/cgi/content/full/jgp.201110706/DC1

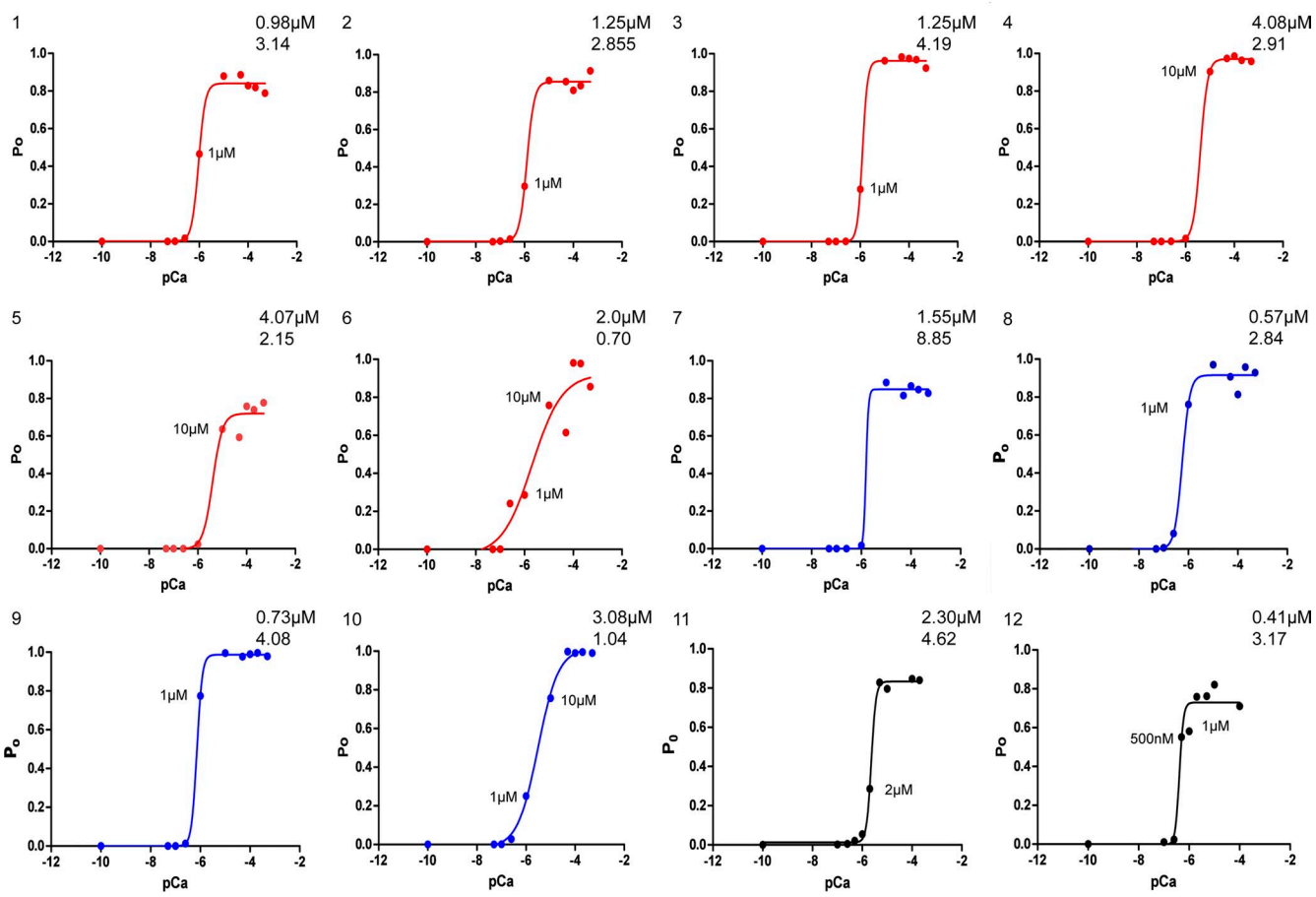

Figure S1. Ca^{2+} activation profiles for 12 hRyR2 channels (0–500 μM). These are color coded as follows: red, channels recorded at 0, 0.05, 0.1, 0.25, 1, 10, 50, 100, 200, and 500 μM $[Ca^{2+}]_{cyt}$, which were all analyzed by MIL fitting; blue, channels recorded at the same concentrations as above, but data either showed periods of modal gating at $P_o \geq 0.8$ resulting in increased T_o values (channels 8, 9, and 10; see Fig. 2 C in main text) or did not exhibit any intermediate open probabilities (channel 7) and were therefore not included in any further analysis; black, channels recorded at additional intermediate concentrations (0, 0.1, 0.25, 0.5, 1, 2, 5, 10, and 100 μM $[Ca^{2+}]_{cyt}$, and 200 μM for channel 11), which were also analyzed by MIL fitting. Individual EC_{50} and Hill coefficient measurements are given in each top right-hand corner.

A

		Actual data	Model demonstrating ligand-dependent rates		Simulated data
200μM	P_o	0.82	$C_{NR} \rightleftharpoons C_R \rightleftharpoons O_1 \rightleftharpoons O_2 \rightleftharpoons O_3 \rightleftharpoons O_4$	P_o	0.8
	T_o	1.65	$\Downarrow\Uparrow$	T_o	1.5
	T_c	0.45	C_F	T_c	0.4
100μM	P_o	0.82	$C_{NR} \rightleftharpoons C_R \rightleftharpoons O_1 \rightleftharpoons O_2 \rightleftharpoons O_3 \rightleftharpoons O_4$	P_o	0.79
	T_o	1.8	$\Downarrow\Uparrow$	T_o	1.2
	T_c	0.35	C_F	T_c	0.4
1μM	P_o	0.45	$C_{NR} \rightleftharpoons C_R \rightleftharpoons O_1 \rightleftharpoons O_2 \rightleftharpoons O_3 \rightleftharpoons O_4$	P_o	0.42
	T_o	1.8	$\Downarrow\Uparrow$	T_o	1.5
	T_c	2.35	C_F	T_c	0.7
0.25μM	P_o	0.02	$C_{NR} \rightleftharpoons C_R \rightleftharpoons O_1 \rightleftharpoons O_2 \rightleftharpoons O_3 \rightleftharpoons O_4$	P_o	0.026
	T_o	0.35	$\Downarrow\Uparrow$ O_{UL} ✗	T_o	0.6
	T_c	18.75	C_F	T_c	29

B

		Actual data	Model demonstrating ligand-dependent rates		Simulated data
200μM	P_o	0.815	$C_{NR} \rightleftharpoons C_R \rightleftharpoons O_1 \rightleftharpoons O_2 \rightleftharpoons O_3 \rightleftharpoons O_4$	P_o	0.93
	T_o	1.75	$\Downarrow\Uparrow$	T_o	2.4
	T_c	0.45	C_F	T_c	0.3
100μM	P_o	0.82	$C_{NR} \rightleftharpoons C_R \rightleftharpoons O_1 \rightleftharpoons O_2 \rightleftharpoons O_3 \rightleftharpoons O_4$	P_o	0.90
	T_o	1.7	$\Downarrow\Uparrow$	T_o	1.7
	T_c	0.4	C_F	T_c	0.3
1μM	P_o	0.339	$C_{NR} \rightleftharpoons C_R \rightleftharpoons O_1 \rightleftharpoons O_2 \rightleftharpoons O_3 \rightleftharpoons O_4$	P_o	0.399
	T_o	1.75	$\Downarrow\Uparrow$	T_o	1.9
	T_c	3.35	C_F	T_c	0.7
0.25μM	P_o	0.0219	$C_{NR} \rightleftharpoons C_R \rightleftharpoons O_1 \rightleftharpoons O_2 \rightleftharpoons O_3 \rightleftharpoons O_4$	P_o	0.025
	T_o	0.45	✗	T_o	1.05
	T_c	34.1	C_F	T_c	30.45

C

		Actual data	Model demonstrating ligand-dependent rates		Simulated data
200μM	P_o	0.840	$C_{NR} \rightleftharpoons C_R \rightleftharpoons O_1 \rightleftharpoons O_2 \rightleftharpoons O_3$	P_o	0.833
	T_o	1.95	$\Downarrow\Uparrow$	T_o	1.0
	T_c	0.3	C_F	T_c	0.25
100μM	P_o	0.846	$C_{NR} \rightleftharpoons C_R \rightleftharpoons O_1 \rightleftharpoons O_2 \rightleftharpoons O_3$	P_o	0.814
	T_o	2.0	$\Downarrow\Uparrow$	T_o	0.75
	T_c	0.5	C_F	T_c	0.3
1μM	P_o	0.054	$C_{NR} \rightleftharpoons C_R \rightleftharpoons O_1 \rightleftharpoons O_2 \rightleftharpoons O_3$	P_o	0.12
	T_o	0.5	$\Downarrow\Uparrow$	T_o	1.5
	T_c	12.4	C_F	T_c	11.8
0.25μM	P_o	0.021	$C_{NR} \rightleftharpoons C_R \rightleftharpoons O_1 \rightleftharpoons O_2 \rightleftharpoons O_3$	P_o	0.038
	T_o	0.45	$\Downarrow\Uparrow$ O_{UL} ✗	T_o	1.275
	T_c	26.9	C_F	T_c	32.75

D

		Actual data	Model demonstrating ligand-dependent rates		Simulated data
200μM	P_o			P_o	
	T_o	No data		T_o	No data
	T_c			T_c	
100μM	P_o	0.82	$C_{NR} \rightleftharpoons C_R \rightleftharpoons O_1 \rightleftharpoons O_2 \rightleftharpoons O_3 \rightleftharpoons O_4$	P_o	0.83
	T_o	1.7	$\Downarrow\Uparrow$	T_o	0.9
	T_c	0.45	C_F	T_c	0.35
1μM	P_o	0.588	$C_{NR} \rightleftharpoons C_R \rightleftharpoons O_1 \rightleftharpoons O_2 \rightleftharpoons O_3 \rightleftharpoons O_4$	P_o	0.36
	T_o	1.25	$\Downarrow\Uparrow$	T_o	1.45
	T_c	1.65	C_F	T_c	1.1
0.25μM	P_o	0.024	$C_{NR} \rightleftharpoons C_R \rightleftharpoons O_1 \rightleftharpoons O_2 \rightleftharpoons O_3 \rightleftharpoons O_4$	P_o	0.018
	T_o	0.3	$\Downarrow\Uparrow$ O_{UL} ✗	T_o	0.4
	T_c	12.9	C_F	T_c	16.2

Figure S2. Dependence of backward as well as forward rates on ligand concentration denotes possible ligand-dependent inhibition at high $[Ca^{2+}]_{cyt}$. Panels show P_o, T_o, and T_c from actual and simulated data. Simulations were performed using the 10-μM model for four channels from Fig. S1: A, channel 1; B, channel 2; C, channel 11; D, channel 12 (where data at 200 μM $[Ca^{2+}]_{cyt}$ was not available). All models apart from that in C achieve four ligand-bound open states. Rates shown in bold were constrained to be linearly dependent on ligand concentration, whereas the others remained fixed. At high $[Ca^{2+}]_{cyt}$ (100–200 μM), making both forward and backward rates from C_R to O_3 or O_4 ligand dependent simulates data comparable to that acquired, suggesting inhibition at these concentrations. At intermediate $[Ca^{2+}]_{cyt}$ (1 μM), ligand dependency of forward (from C_R to O_3 or O_4) and backward rates between open states only (i.e., from O_1 to O_3 or O_4) simulates data similar to that obtained in practice. At low (0.25 μM) $[Ca^{2+}]_{cyt}$, ligand dependence of forward rates (from C_R to O_3 or O_4) only simulates data comparable to that recorded. At this $[Ca^{2+}]_{cyt}$, the addition of O_{UL} (using fixed-rate constants from the individual channel, if this state was resolved, as in A, C, and D), and the removal of C_F further improved the match between actual and simulated data.